

doi:10.3788/gzxb20174611.1122004

折/衍混合大视场消热差红外双波段光学系统设计

陶 郅¹, 王 敏¹, 肖 维 军², 郭 王 凯¹

(1 福建师范大学 光电与信息工程学院 福建省光子技术重点实验室 教育部医学光学重点实验室,
福州 350007)

(2 福建福光股份有限公司, 福州 350007)

摘 要:根据双波段消热差理论设计了大视场消热差红外双波段光学系统.系统为 4 片式反远结构,包括一个衍射面和一个非球面,设计波长为 $3.5\sim 4.8\ \mu\text{m}/8\sim 12\ \mu\text{m}$,焦距为 8 mm,全视场 80.2° , $F/\#$ 为 2,系统出瞳与冷光阑严格匹配,满足 100%冷光阑效率.根据消热差条件和波段间消色差条件,得出 4 片分离薄透镜光焦度分配的解,进一步建立了三维投影消热差图,据此合理选择光学材料.根据环境温度要求,利用光学被动式消热差的方法实现了系统在 $-40\sim 60^\circ\text{C}$ 的温度变化范围内的消热差设计.结果表明,系统在环境温度变化范围内成像质量良好,实现了光学系统无热化.

关键词:光学设计;双波段;消热差;折/衍混合;大视场

中图分类号:TN216

文献标识码:A

文章编号:1004-4213(2017)11-1122004-9

Design for Cooled Dual-band Infrared Refractive-Diffractive Hybrid Optical System of Athermalization and Wide FOV

TAO Zhi¹, WANG Min¹, XIAO Wei-jun², GUO Wang-kai¹

(1 College of Photonic and Electronic Engineering, Fujian Normal University, Fujian Provincial Key Lab of Photonic Technology; Key Laboratory of Optoelectronic Science and Technology for Medicine of Ministry of Education, Fuzhou 350007, China)

(2 Fujian Forecam Optics Co., Ltd., Fuzhou 350007, China)

Abstract: On the basis of the dual-band athermal theory, a cooled dual-band infrared refractive-diffractive hybrid optical system of athermalized and wide field of view was designed. The system consists of 4 lenses and introduces only 1 diffractive surface and 1 aspherical surface, the full field of view is 80.2° , the focal length is 8 mm, F number is 2, the operating wavelength range is $3.5\sim 4.8\ \mu\text{m}$ and $8\sim 12\ \mu\text{m}$, and the cold stop efficiency is 100%. The solutions of 4 separate thin lenses were obtained by analyzing dual-band achromatic and athermalized theory. Further, establishing the material model of athermalized dual-band optic system and choosing the optical materials properly. According to requirements, the dual-band athermal optical system with temperature of -40°C to 60°C was designed with the use of optical passive. The results prove that the optical system obtains a good image quality during -40°C to 60°C , and realizes athermalization.

Key words: Optical design; Dual-band; Athermalization; Refractive/diffractive hybrid; Wide field of view

OCIS Codes: 040.3060; 080.2740; 080.3620; 080.6755; 090.1970

0 引言

大气中同一个目标物体在不同波段有不同的辐射特性,其中短波红外与可见光较为相似.在湿热的环境

基金项目:国家自然科学基金(No.61520106015)资助

第一作者:陶郅(1990-),男,硕士研究生,主要研究方向为光学系统设计. Email: taozhieu@163.com

导师(通讯作者):王敏(1963-),女,教授级高级工程师,主要研究方向为光学镜头及精密仪器. Email: mwang@fjnu.edu.cn

收稿日期:2016-12-29;录用日期:2017-05-17

<http://www.photon.ac.cn>

中,波长为 $3\sim 5\mu\text{m}$ 的中波红外(Mid-Wavelength Infrared, MWIR)的侦查能力较为优越,主要用于观测高温事件;波长为 $8\sim 12\mu\text{m}$ 的长波红外(Long-Wavelength Infrared, LWIR)在存在杂散辐射或靠近热源的情况下具有较强的侦查能力,主要用于探测常温物体轮廓^[1-2].多波段光学系统的优势是具有全天候观察的能力,分辨率高、采集光信息量大,可以应用于雾霾、沙尘等诸多复杂环境条件中,在许多自然灾害后的救援工作中发挥着重要作用.

随着双色红外探测器的发展,双波段红外光学系统的研究也在不断深入,能在同一个光学系统中观察不同类型目标、不同环境条件、不同识别任务^[3-5].目前,对红外中波长波段同时敏感的探测器阵列主要有双波段碲镉汞焦平面阵列和量子阱红外光电探测器阵列^[6].双波段共焦光学系统能同时采集两种波长,在同一像面位置得到稳定的像质.温度变化会引起像差和热离焦,需要对设计进行无热化处理.

自 20 世纪 70 年代法国研制出双波段红外光学系统 VAMPIR 至今^[7],运用各种方法设计的双波段红外消热差光学系统已经取得了丰富的成果.张欣婷等在光学系统中引入双层衍射元件,利用衍射元件负色散的特性和光热膨胀系数小的特性,同时消色差和消热差^[7];常军等采用离轴反射结构设计光学无热化系统^[8];贾永丹等在双视场/双色红外消热差光学系统设计中使用投影消热差图合理选择光学材料^[9];杨新军等通过计算消热差消色差方程,合理分配光焦度^[10],付强等提出了计算多个波长下平均离焦的方法^[11]实现红外双波段无热化.

本文研究了光学被动式消热差条件、波段间消色差条件,建立了新三维消热差图(TPC图).设计了 4 片折/衍混合结构的大视场(Field of View, FOV)双波段共焦消热差光学系统,仅使用了一面非球面和一面衍射面.系统采用了制冷型双波段探测器,实现了 100%冷光阑效率,满足消除背景杂光的要求.系统总长小于 84 mm,光阑距离像面 20 mm,后截距大于 12 mm,在 $-40\sim 60^\circ\text{C}$ 实现了消热差,即温度导致的像面移动在焦深范围内.

1 设计思路及理论分析

1.1 红外双波段波段间消色差原理

分别在中波长波段应用物像关系公式有

$$\frac{1}{l'_{1c}} - \frac{1}{l_{1c}} = (n_{1c} - 1) \left(\frac{1}{R_1} - \frac{1}{R_2} \right) = \varphi_{1c} \quad (1)$$

$$\frac{1}{l'_{2c}} - \frac{1}{l_{2c}} = (n_{2c} - 1) \left(\frac{1}{R_1} - \frac{1}{R_2} \right) = \varphi_{2c} \quad (2)$$

式中, l_{1c} 、 l'_{1c} 、 n_{1c} 、 φ_{1c} 分别表示长波波段中心波长的物距、像距、折射率、光焦度, l_{2c} 、 l'_{2c} 、 n_{2c} 、 φ_{2c} 分别表示中波波段中心波长的物距、像距、折射率、光焦度, R_1 、 R_2 为元件曲率半径.

对式(1)、(2)作一阶近似得

$$\frac{l'_{2c} - l'_{1c}}{l'^2} - \frac{l_{2c} - l_{1c}}{l^2} = (n_{1c} - n_{2c}) \left(\frac{1}{R_1} - \frac{1}{R_2} \right) = \frac{(n_{1c} - n_{2c})}{(n_{1c} - 1)} \varphi_{1c} \quad (3)$$

类比阿贝数定义,取 $\frac{(n_{1c} - n_{2c})}{(n_{1c} - 1)} = P$ 为波段间色系数,波段间色差为 $L'_{pk} = l'_{2c} - l'_{1c}$,则^[12]

$$L'_{pk} = \frac{1}{u^2} \sum y_k^2 P_k \varphi_k = \frac{1}{(h_1 \varphi)^2} \sum y_k^2 P_k \varphi_k \quad (4)$$

式中, L'_{pk} 为系统迭加波段间色差, y_k 表示第 k 面光线高度.

1.2 红外双波段消热差原理

薄透镜光焦度公式为

$$\varphi = (n - n_0)(c_1 - c_2) \quad (5)$$

微分可得

$$\frac{d\varphi}{dT} = \left(\frac{dn}{dT} - \frac{dn_0}{dT} \right) (c_1 - c_2) + (n - n_0) \left(\frac{dc_1}{dT} - \frac{dc_2}{dT} \right) \quad (6)$$

式中, T 表示温度, n_0 为介质折射率, n 为薄透镜折射率, c_1 、 c_2 为透镜前表面和后表面的曲率.

由光学材料热膨胀系数为

$$\alpha_g = c_1^{-1} \frac{dc_1}{dT} = c_2^{-1} \frac{dc_2}{dT} \quad (7)$$

可得透射薄透镜的光热离焦系数为^[13]

$$T_{f,r} = \alpha_g - \frac{1}{n-n_0} \left(\frac{dn}{dT} - \frac{dn_0}{dT} \right) \quad (8)$$

从式(8)可以看出,折射元件的光热离焦系数只由玻璃材料性质决定.

衍射光学元件光热离焦系数为^[14]

$$T_{f,D} = \frac{1}{f} \frac{df}{dT} = 2\alpha_g + \frac{1}{n_0} \frac{dn_0}{dT} \quad (9)$$

式中, f 为光焦度 φ 对应的焦距,从式(9)可以看出,衍射元件的光热离焦系数只与玻璃材料的光热膨胀系数 α_g 有关.由表 1 中中波红外材料的折射率温度变化梯度 $\frac{dn}{dT}$,和长波红外材料的折射率温度变化梯度 $\frac{dn}{dT}$ 可知薄透镜的光热离焦系数小于零,衍射光学元件光热离焦系数大于零,机械材料的热膨胀系数大于零.故本系统采用光学被动消热差的办法,即透射元件的光热离焦量、衍射元件的光热离焦的综合离焦与机械材料的热膨胀离焦量相互补偿,使光学系统的像面离焦量在焦深范围内.双波段红外光学系统无热化,要满足五个方程:

系统光焦度方程为

$$\sum_{i=1}^j h_i \phi_i = \phi \quad (10)$$

中波波段内消色差为

$$\left(\frac{1}{h_1 \phi} \right)^2 \sum_{i=1}^j h_i^2 C_{mi} \phi_i = \Delta f_{1b} \quad (11)$$

长波波段内消色差为

$$\left(\frac{1}{h_1 \phi} \right)^2 \sum_{i=1}^j h_i^2 C_{li} \phi_i = \Delta f_{2b} \quad (12)$$

消热差条件为

$$\alpha_H L = \left(\frac{1}{h_1 \phi} \right)^2 \sum_{i=1}^j h_i^2 T_i \phi_i \quad (13)$$

波段间消色差为

$$L'_p = \frac{1}{(h_1 \phi)^2} \sum h_i^2 P_i \phi_i \quad (14)$$

其中 φ 为系统的总光焦度, h_i 为第一近轴光线在第 i 个透镜上的入射高度, ϕ_i 每个透镜的光焦度, C_{mi} 是第 i 个透镜材料在中波红外波段的色散因子, C_{li} 是第 i 个透镜材料在长波红外波段的色散因子, T_i 是第 i 个透镜的光热离焦系数.

1.3 红外材料特性及选取

表 1 列出中波红外、长波红外常用材料,及其对应的应用波段范围、光学性质、热学性质^[15-16].

表 1 光学材料的中波红外特性和长波红外特性

Table 1 Material properties of mid-wavelength infrared and long-wavelength infrared

| Character/ trademark | Refractive index at 4 μm | Refractive index at 10 μm | Abbe number 10 μm (8-12 μm) | Abbe number 4 μm (3-5 μm) | Inter band chromatic aberration/ ($\times 10^{-3}$) | Thermal dispersive power/ ($\times 10^{-6}/\text{K}$) | dn/dt at 4 $\mu\text{m}/$ ($\times 10^{-6}/\text{K}$) | dn/dt at 10 $\mu\text{m}/$ ($\times 10^{-6}/\text{K}$) |
|-------------------------|---|--|--|--|--|--|---|--|
| Ge | 4.024 3 | 4.032 | 783.394 3 | 116.315 | 6.836 | 12.61 | 396 | 396 |
| ZnSe | 2.433 2 | 2.406 4 | 57.468 92 | 177.988 | 18.646 | 37.7 | 60 | 61 |
| ZnS | 2.252 5 | 2.199 9 | 22.756 17 | 109.635 | 41.965 | 30.2 | 38.7 | 44 |
| AMTIR-1 | 2.514 1 | 2.497 6 | 113.116 5 | 172.337 8 | 11.197 451 | 36.1 | 79 | 70.5 |
| IG4 | 2.620 9 | 2.608 2 | 172.436 | 194.922 6 | 9.431 56 | 20.4 | 92 | 91 |
| IG6 | 2.794 5 | 2.777 7 | 160.118 | 168.091 1 | 3.108 059 | 16 | 76 | 76 |

分析密接两组元系统,有

$$\begin{cases} \varphi_1 + \varphi_2 = \phi \\ \frac{C_{m1}\varphi_1 + C_{m2}\varphi_2}{\phi} = 0 \\ \frac{C_{l1}\varphi_1 + C_{l2}\varphi_2}{\phi} = 0 \\ \frac{T_1\varphi_1 + T_2\varphi_2}{\phi} = 0 \\ P_1\varphi_1 + P_2\varphi_2 = 0 \end{cases} \quad (15)$$

其解为

$$\begin{cases} \varphi_1 = \frac{C_{m2}\varphi}{C_{m2} - C_{m1}} = -\frac{C_{l2}\varphi}{C_{l2} - C_{l1}} = \frac{T_2\varphi}{T_2 - T_1} = \frac{P_2\varphi}{P_2 - P_1} \\ \varphi_2 = -\frac{C_{m1}\varphi}{C_{m2} - C_{m1}} = -\frac{C_{l1}\varphi}{C_{l2} - C_{l1}} = -\frac{T_1\varphi}{T_2 - T_1} = \frac{-P_2\varphi}{P_2 - P_1} \end{cases} \quad (16)$$

方程有解的条件是 $\frac{C_{m2}}{C_{m1}} = \frac{C_{l2}}{C_{l1}} = \frac{T_2}{T_1} = \frac{P_2}{P_1}$.

分析密接四组元系统,有

$$\begin{cases} \varphi_1 + \varphi_2 + \varphi_3 + \varphi_4 = \phi \\ \frac{C_{m1}\varphi_1 + C_{m2}\varphi_2 + C_{m3}\varphi_3 + C_{m4}\varphi_4}{\phi} = 0 \\ \frac{C_{l1}\varphi_1 + C_{l2}\varphi_2 + C_{l3}\varphi_3 + C_{l4}\varphi_4}{\phi} = 0 \\ \frac{T_1\varphi_1 + T_2\varphi_2 + T_3\varphi_3 + T_4\varphi_4}{\phi} = 0 \\ P_1\varphi_1 + P_2\varphi_2 + P_3\varphi_3 + P_4\varphi_4 = 0 \end{cases} \quad (17)$$

其解为

$$\begin{cases} \varphi_1 = \frac{P_2(C_{m3}T_4 - C_{m4}T_3) + P_3(T_2C_{m4} - C_{m2}T_4) + P_4(C_{m2}T_3 - T_2C_{m3})}{N_1} = \\ \frac{P_2(C_{l3}T_4 - C_{l4}T_3) + P_3(T_2C_{l4} - C_{l2}T_4) + P_4(C_{l2}T_3 - T_2C_{l3})}{N_2} \\ \varphi_2 = \frac{P_1(C_{m3}T_4 - C_{m4}T_3) + P_3(T_1C_{m4} - C_{m1}T_4) + P_4(C_{m1}T_3 - T_1C_{m3})}{N_1} = \\ \frac{P_1(C_{l3}T_4 - C_{l4}T_3) + P_3(T_1C_{l4} - C_{l1}T_4) + P_4(C_{l1}T_3 - T_1C_{l3})}{N_2} \\ \varphi_3 = \frac{P_1(C_{m2}T_4 - C_{m4}T_2) + P_2(T_1C_{m4} - C_{m2}T_4) + P_4(C_{m1}T_2 - T_1C_{m2})}{N_1} = \\ \frac{P_1(C_{l2}T_4 - C_{l4}T_2) + P_2(T_1C_{l4} - C_{l2}T_4) + P_4(C_{l1}T_2 - T_1C_{l2})}{N_2} \\ \varphi_4 = \frac{P_1(C_{m2}T_3 - C_{m3}T_2) + P_2(T_1C_{m3} - C_{m2}T_3) + P_3(C_{m1}T_2 - T_1C_{m2})}{N_1} = \\ \frac{P_1(C_{l2}T_3 - C_{l3}T_2) + P_2(T_1C_{l3} - C_{l2}T_3) + P_3(C_{l1}T_2 - T_1C_{l2})}{N_2} \end{cases} \quad (18)$$

其中,

$$\begin{cases} N_1 = P_1(C_{m4}T_3 - C_{m3}T_4 + C_{m2}T_4 - C_{m4}T_2 + C_{m2}T_3 - C_{m3}T_2) + P_2(C_{m1}T_4 - C_{m4}T_1 + C_{m1}T_3 - \\ C_{m3}T_1 + C_{m3}T_4 - C_{m4}T_3) + P_3(C_{m1}T_4 - C_{m4}T_1 + C_{m1}T_2 - C_{m2}T_1 + C_{m2}T_4 - C_{m4}T_2) + \\ P_4(C_{m1}T_2 - C_{m2}T_1 + C_{m1}T_3 - C_{m3}T_1 + C_{m2}T_3 - C_{m3}T_2) \end{cases}$$

$$\begin{cases} N_2 = P_1(C_{14}T_3 - C_{13}T_4 + C_{12}T_4 - C_{14}T_2 + C_{12}T_3 - C_{13}T_2) + P_2(C_{11}T_4 - C_{14}T_1 + C_{11}T_3 - \\ C_{13}T_1 + C_{13}T_4 - C_{14}T_3) + P_3(C_{11}T_4 - C_{14}T_1 + C_{11}T_2 - C_{12}T_1 + C_{12}T_4 - C_{14}T_2) + \\ P_4(C_{11}T_2 - C_{12}T_1 + C_{11}T_3 - C_{13}T_1 + C_{12}T_3 - C_{13}T_2) \end{cases} \quad (19)$$

式(10)~(14)中,取 $h_i\varphi_i = \varphi'_i, h_iT_i = T'_i, h_iC_i = C'_i$,分析分离四组元系统,得

$$\begin{cases} \varphi'_1 + \varphi'_2 + \varphi'_3 + \varphi'_4 = \phi \\ \frac{C'_{m1}\varphi'_1 + C'_{m2}\varphi'_2 + C'_{m3}\varphi'_3 + C'_{m4}\varphi'_4}{\phi} = 0 \\ \frac{C'_{11}\varphi'_1 + C'_{12}\varphi'_2 + C'_{13}\varphi'_3 + C'_{14}\varphi'_4}{\phi} = 0 \\ \frac{T'_1\varphi'_1 + T'_2\varphi'_2 + T'_3\varphi'_3 + T'_4\varphi'_4}{\phi} = 0 \\ \frac{P'_1\varphi'_1 + P'_2\varphi'_2 + P'_3\varphi'_3 + P'_4\varphi'_4}{\phi} = 0 \end{cases} \quad (20)$$

其解为

$$\begin{cases} \varphi'_1 = \frac{P'_2(C'_{m3}T'_4 - C'_{m4}T'_3) + P'_3(T'_2C'_{m4} - C'_{m2}T'_4) + P'_4(C'_{m2}T'_3 - T'_2C'_{m3})}{N_1} = \\ \frac{P'_2(C'_{13}T'_4 - C'_{14}T'_3) + P'_3(T'_2C'_{14} - C'_{12}T'_4) + P'_4(C'_{12}T'_3 - T'_2C'_{13})}{N_2} \\ \varphi'_2 = \frac{P'_1(C'_{m3}T'_4 - C'_{m4}T'_3) + P'_3(T'_1C'_{m4} - C'_{m1}T'_4) + P'_4(C'_{m1}T'_3 - T'_1C'_{m3})}{N_1} = \\ \frac{P'_1(C'_{13}T'_4 - C'_{14}T'_3) + P'_3(T'_1C'_{14} - C'_{11}T'_4) + P'_4(C'_{11}T'_3 - T'_1C'_{13})}{N_2} \\ \varphi'_3 = \frac{P'_1(C'_{m2}T'_4 - C'_{m4}T'_2) + P'_2(T'_1C'_{m4} - C'_{m2}T'_4) + P'_4(C'_{m1}T'_2 - T'_1C'_{m2})}{N_1} = \\ \frac{P'_1(C'_{12}T'_4 - C'_{14}T'_2) + P'_2(T'_1C'_{14} - C'_{12}T'_4) + P'_4(C'_{11}T'_2 - T'_1C'_{12})}{N_2} \\ \varphi'_4 = \frac{P'_1(C'_{m2}T'_3 - C'_{m3}T'_2) + P'_2(T'_1C'_{m3} - C'_{m2}T'_3) + P'_3(C'_{m1}T'_2 - T'_1C'_{m2})}{N_1} = \\ \frac{P'_1(C'_{12}T'_3 - C'_{13}T'_2) + P'_2(T'_1C'_{13} - C'_{12}T'_3) + P'_3(C'_{11}T'_2 - T'_1C'_{12})}{N_2} \end{cases} \quad (21)$$

其中

$$\begin{cases} N_1 = P'_1(C'_{m4}T'_3 - C'_{m3}T'_4 + C'_{m2}T'_4 - C'_{m4}T'_2 + C'_{m2}T'_3 - C'_{m3}T'_2) + P'_2(C'_{m1}T'_4 - C'_{m4}T'_1 + C'_{m1}T'_3 - \\ C'_{m3}T'_1 + C'_{m3}T'_4 - C'_{m4}T'_3) + P'_3(C'_{m1}T'_4 - C'_{m4}T'_1 + C'_{m1}T'_2 - C'_{m2}T'_1 + C'_{m2}T'_4 - C'_{m4}T'_2) + \\ P'_4(C'_{m1}T'_2 - C'_{m2}T'_1 + C'_{m1}T'_3 - C'_{m3}T'_1 + C'_{m2}T'_3 - C'_{m3}T'_2) \\ N_2 = P'_1(C'_{14}T'_3 - C'_{13}T'_4 + C'_{12}T'_4 - C'_{14}T'_2 + C'_{12}T'_3 - C'_{13}T'_2) + P'_2(C'_{11}T'_4 - C'_{14}T'_1 + C'_{11}T'_3 - \\ C'_{13}T'_1 + C'_{13}T'_4 - C'_{14}T'_3) + P'_3(C'_{11}T'_4 - C'_{14}T'_1 + C'_{11}T'_2 - C'_{12}T'_1 + C'_{12}T'_4 - C'_{14}T'_2) + \\ P'_4(C'_{11}T'_2 - C'_{12}T'_1 + C'_{11}T'_3 - C'_{13}T'_1 + C'_{12}T'_3 - C'_{13}T'_2) \end{cases} \quad (22)$$

在初始解中为减小系统的高级像差,应尽量减小各组元的光焦度.由式(18)和(21)可以看出,分母越大,各组元的光焦度越小,即 N_1, N_2 越小,系统各组元的光焦度越小.根据分析建立三维坐标系, X 轴为 C, Y 轴为 T, Z 轴为 P .在同一坐标系中标记出各个材料在 $3\sim 5 \mu\text{m}$ 波段内各性能指标的散点图(Δ)和 $8\sim 12 \mu\text{m}$ 波段内各性能指标的散点图(O).根据表 1 在图 1 中标出各个材料,绘制出其中三种材料组成的新型消热差 TPC 图,如图 1.以长波下的三种材料所组成的三角形为基准平面,将中波下的三角形投影到基准平面上.其重合面积越大,系统初始结构时分配到各个元件的光焦度越小,对像质越有利.

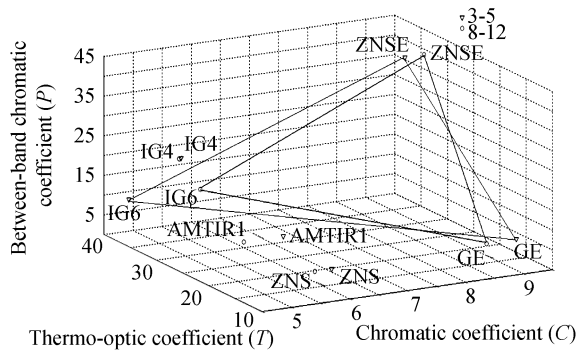


图1 双波段消热差 TPC 图
Fig.1 TPC diagram of dual-band athermalization

2 设计实例

表 2 列出了制冷型双波段消热差光学系统和大视场长波红外消热差光学系统的设计方法与指标. 基于一款像面尺寸为 384×288 , 像元尺寸为 $25 \mu\text{m}$ 的制冷型双波段红外探测器, 设计参数见表 3. 系统共采 2 片 GE, 1 片 ZNSE, 1 片 IG4 材料, 系统 $F/\#$ 为 2, 将光阑后置于光学系统后, 探测器窗口前, 出瞳大小和冷屏大小配合, 满足 100% 的冷光阑效率. 根据新三维投影热差图选择光学材料, 合理分配光焦度, 使用光学仿真软件 ZEMAX 优化光学系统, 最终得到光学系统结构如图 2. 系统为反远结构, 主面后移, 后截距大于 12 mm. 第一面的相对孔径大, 轴外光线高度高. 第一片透镜为负光焦度大折射率的 GE 材料, 有利于大视场下光线的偏折, GE 材料的波段内色散和波段间色散都很小, 不产生大的像差. 第二片为正光焦度透镜, 在第二片透镜的后表面引入一面二元衍射面平衡色差, 负色散的衍射元件有利于消除色差, 减小镜片的曲率和所承担的光焦度. 第三片透镜为负光焦度的 ZnSe. 第四片透镜的材料为 GE 材料, 在四片透镜的前表面引入一面非球面, 校正大视场引起的轴外剩余像差, 以及剩余色差.

表 2 制冷型定焦红外消热差系统的指标和主要设计方法

Table 2 Design index and method of cooled infrared optical system of athermalized

| Reference | Wavelength/ μm | FOV/ ($^\circ$) | $F/\#$ | Effective focal length/mm | Detector | The total number of lens(PCS) | Total length/ mm | Major technique |
|----------------|------------------------------|----------------------|--------|------------------------------|--|----------------------------------|---------------------|---|
| No.1 | 3.5-4.8/ 9.2-10.8 | 74 | 2.5 | 9.5 | $384 \times 288 /$ $25 \mu\text{m}$ | 3 | 202 | Three mirror unobscured system |
| No.2 | 3.5~4.8/ 8~12 | 68 | 2 | 10 | $384 \times 288 /$ $25 \mu\text{m}$ | 5 | 113 | Refractive system with 3 aspheric surfaces |
| No.3 | 4.4~5.7 7.8~8.8 | 96 | 4 | 6 | $384 \times 288 /$ $25 \mu\text{m}$ | 6 | 62 | Double-layer harmonic diffraction element |
| No.4 | 3-5 | 82 | 2 | 8 | $384 \times 288 /$ $25 \mu\text{m}$ | 3 | 65 | Refractive-Diffractive Hybrid System |
| This design | 3.5~4.8/ 8~12 | 80.2 | 2 | 8 | $384 \times 288 /$ $25 \mu\text{m}$ | 4 | 84 | Refractive-Diffractive Hybrid System |

表 3 系统设计参数

Table 3 System design parameters

| Parameters | Value |
|---|--------------|
| Wavelength/ μm | 3.5-4.8 8-12 |
| FOV/ $^\circ$ | 80.2 |
| Effective focal length/mm | 8 |
| $F/\#$ | 2 |
| Cold shield efficiency | 100% |
| Operating temperature/ $^\circ\text{C}$ | -40~60 |

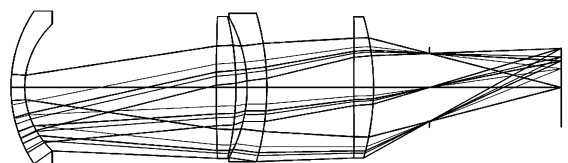


图 2 制冷型红外双波段消热差系统结构
Fig.2 Athermalized dual-band infrared optical
system structure

3 设计评价

系统长波星点在衍射极限内,中波星点接近衍射极限,如图 3.中波焦深 $\Delta z = \pm 2\lambda(F/\#) = 64 \mu\text{m}$,长波焦深为 $\Delta z = \pm 2\lambda(F/\#) = 160 \mu\text{m}$,系统最大离焦量为 $62.892 \mu\text{m}$,小于两个波段的焦深,能够实现共焦.系统 MTF 如图 4,在 $-40 \sim 60^\circ\text{C}$ 的温度范围内变化极小,长波 MTF 在 20 lp/mm 大于 0.6,中波 MTF 在 20 lp/mm 大于 0.34,成像质量良好.

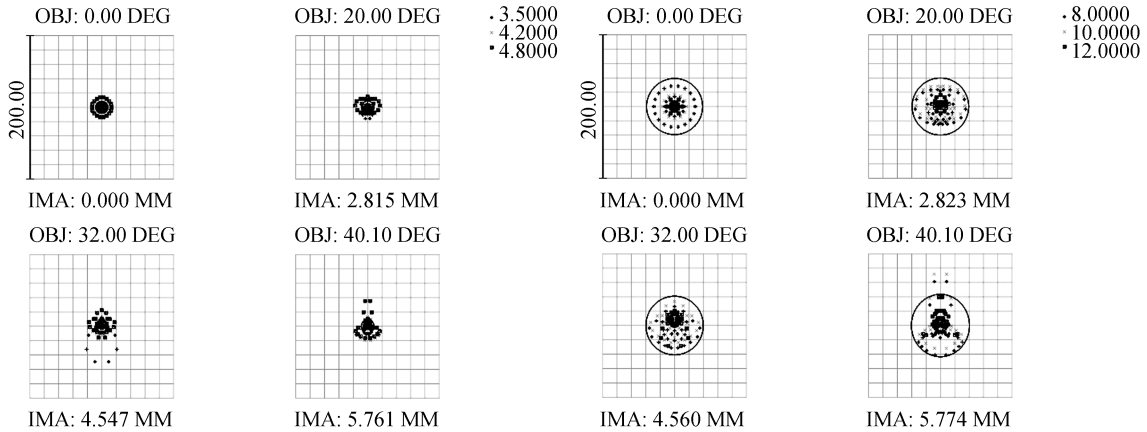
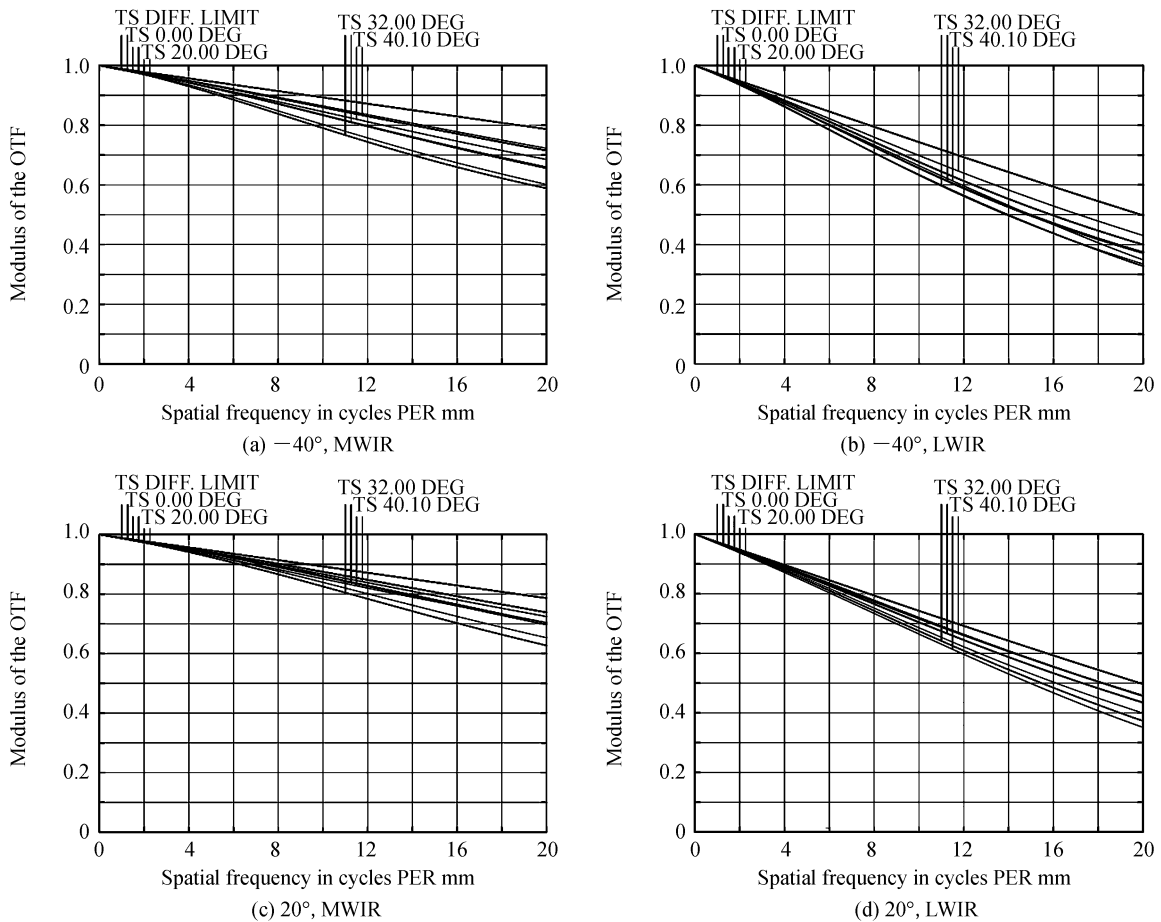


图 3 星点图
Fig.3 Spot diagram



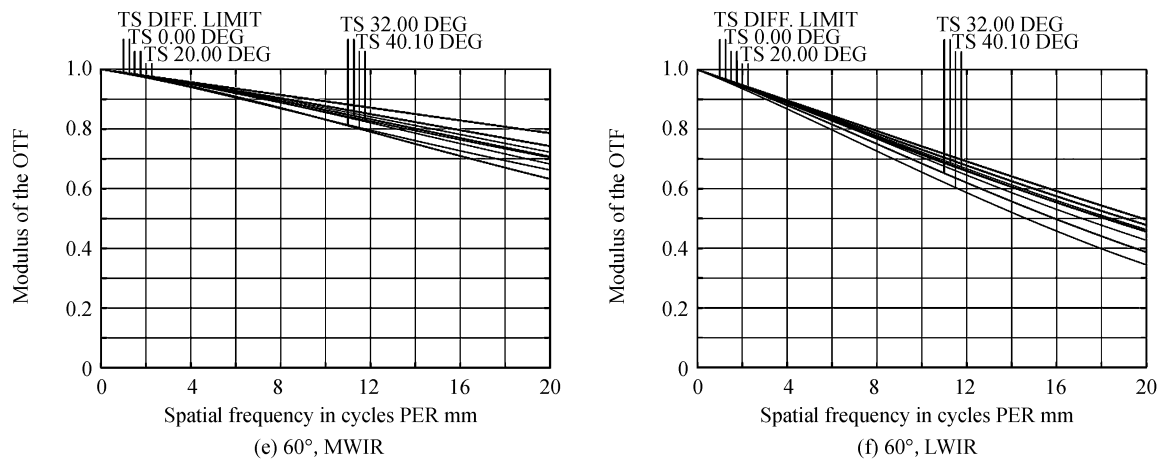


图4 制冷型红外双波段消热差系统 MTF 图
Fig.4 MTF of athermalized dual-band infrared optical system

4 结论

本文分析了红外双波段消热差和消色差条件,结合新三维消热差图合理选择材料,构建了红外双波段消热差光学系统,实现了在 $-40\sim 60^{\circ}\text{C}$ 光学系统无热化设计.运用新型三维消热差图选择材料更加直观,且利于材料重新选择分配.该方法需要逐一对比不同的材料组合,由于红外材料种类少,方法优点明显,可广泛应用于各红外波段的光学设计中.但是,在可见光的双波段消热差设计中,因为可选择的材料多,用新型三维消热差图选择材料效率低.可以采用计算机编写材料分析程序,对大量光学材料作选择对比,结合理论进一步扩展该方法在可见光领域的应用.

参考文献

- [1] JAMIESONT H. Ultra wide waveband optics[J]. *Optical Engineerng*, 1984, **23**(2):10-16.
- [2] JIANG H, QIAN Y, RHEE K T. High speed dual spectral infrared imaging[J]. *Optical Engineerng*, 1993, **32**(6): 1281-283.
- [3] SUN Qiang, LU Zhen-wu, WANG Zhao-qi. The dual band design of harmonic diffractive-refractive optics system[J]. *Acta Optica Sinica*, 2004, **24**(6): 830-833.
孙强, 卢振武, 王肇圻. 谐波衍射/折射双波段系统设计[J]. *光学学报*, 2004, **24**(6): 830-833.
- [4] SCHREER O. Helicopter-borne dual-band dual-FPA system[C]. Proceedings of SPIE-The International Society for Optical Engineering, 2003, **5074**: 637-647.
- [5] WU Hai-qing, WANG Hai-xia, ZHAO Xin-liang, et al. Design of dual-band/dual-field IR optical system[J]. *Infrared Technology*, 2010, **32**(11): 640-644.
吴海清, 王海霞, 赵新亮, 等. 双波段/双视场红外光学系统设计[J]. *红外技术*, 2010, **32**(11): 640-644.
- [6] DING Rui-jun, YE Zhen-hua, ZHOU Wen-bo, et al. Review of two-color infrared focal plane arrays[J]. *Infrared and Laser Engineering*, 2008, **37**(1): 14-17, 29.
丁瑞军, 叶振华, 周文波, 等. 双色红外焦平面研究进展[J]. *红外与激光工程*, 2008, **37**(1): 14-17, 29.
- [7] VIZGAITIS J N, WITTE K, LITTLETON R, et al. Compact dual field of view SWIR/MWIR optical system[C]. SPIE, 2011, 8012: 081225.
- [8] ZHANG Xin-ting, AN Zhi-yong. Design of infrared athermal optical system for dual-band with double-layer harmonic diffraction element[J]. *Acta Optica Sinica*, 2013, **33**(6): 062204.
张欣婷, 安志勇. 双层谐波衍射双波段红外消热差光学系统设计[J]. *光学学报*, 2013, **33**(6): 062204.
- [9] CHANG Jun, LIU Li-ping, WANG Yong-tian, et al. Dual-band infrared optical system with large field-of-view and aperture[J]. *Journal of Infrared and Millimeter Waves*, 2006, **25**(3): 170-172.
常军, 刘莉萍, 王涌天, 等. 大视场、大口径双波段红外非制冷光学系统[J]. *红外与毫米波学报*, 2006, **25**(3): 170-172.
- [10] JIA Yong-dan, FU Yue-gang, LIU Zhi-ying, et al. Athermalization design of dual-band/dual-field infrared optical system[J]. *Acta Photonic Sinica*, 2012, **41**(6): 638-641.
贾永丹, 付跃刚, 刘智颖, 等. 双视场/双色红外消热差光学系统设计[J]. *光子学报*, 2012, **41**(6): 638-641.
- [11] FU Qiang, ZHANG Xin. Materials choose for mid-wave/long-wave dual-band infrared optics[J]. *Acta Optica Sinica*, 2015, **35**(2): 0208003.
付强, 张新. 中波/长波双色红外光学系统材料选择[J]. *光学学报*, 2015, **35**(2): 0208003.

- [12] YANG Xin-jun, WANG Zhao-qi, MU Guo-guang. Athermalization design of infrared dual-band optical system [J]. *Journal of Optoelectronics Laser*, 2004, **15**(4):385-389.
杨新军, 王肇圻, 母国光, 等. 红外双波段消热差系统设计[J]. 光电子·激光, 2004, **15**(4):385-389.
- [13] THOMASH H J T. Effects in optical systems[J]. *Optical Engineering*, 1981, **20**(2):156-160.
- [14] BEHRMANN G P, BOWEN J P. Influence of temperature on diffractive lens performance[J]. *Applied Optics*, 1993, **32**(14):2483-2489.
- [15] XIANG Chang-ming, WEN Shang-sheng, CHEN Ying, *et al.* Optical system design of LED area source for ultraviolet curing [J]. *Chinese Journal of Luminescence*, 2016, **37**(12): 1507-1513.
向昌明, 文尚胜, 陈颖, 等. 紫外光 LED 固化面光源光学系统设计[J]. 发光学报, 2016, **37**(12): 1507-1513.
- [16] YANG Pei-zhi, LIU Li-ming, ZHANG Xiao-wen, *et al.* Research progress of long -wavelength infrared optical materials [J]. *Journal of Inorganic Materials*, 2007, **23**(4): 641-646.
杨培志, 刘黎明, 张小文, 等. 长波红外光学材料的研究进展[J]. 无机材料学报, 2008, **23**(4):641-646.